


ORIGINAL ARTICLE

ARID1A loss induces P4HB to activate fibroblasts to support lung cancer cell growth, invasion, and chemoresistance

Risheng Huang¹  | Danni Wu¹ | Kangliang Zhang² | Guanqiong Hu³ | Yu Liu⁴ | Yi Jiang⁵ | Chichao Wang¹ | Yuanliang Zheng¹

¹Department of Thoracic Surgery, The Dingli Clinical College of Wenzhou Medical University, Wenzhou Central Hospital, Wenzhou, China

²Department of Central Lab, The Dingli Clinical College of Wenzhou Medical University, Wenzhou Central Hospital, Wenzhou, China

³Department of Nursing, The First Affiliated Hospital of Wenzhou Medical University, Wenzhou, China

⁴Department of Thoracic Surgery, The First Affiliated Hospital of Wenzhou Medical University, Wenzhou, China

⁵Department of Pathology, The Dingli Clinical College of Wenzhou Medical University, Wenzhou Central Hospital, Wenzhou, China

Correspondence

Yuanliang Zheng, Department of Thoracic Surgery, The Dingli Clinical College of Wenzhou Medical University, Wenzhou Central Hospital, Wenzhou, China.
Email: fdzyl1989@126.com

Funding information

Collaborative education project of industry university cooperation of the Ministry of Education of China, Grant/Award Number: 202101160012; Key Laboratory of Precision Medicine of Wenzhou of China, Grant/Award Number: 2021HZSY0065; Natural Science Foundation of Zhejiang Province, China, Grant/Award Number: LQ22H160024 and LY21H160011

Abstract

Loss of AT-interacting domain-rich protein 1A (*ARID1A*) frequently occurs in human malignancies including lung cancer. The biological consequence of *ARID1A* mutation in lung cancer is not fully understood. This study was designed to determine the effect of *ARID1A*-depleted lung cancer cells on fibroblast activation. Conditioned media was collected from *ARID1A*-depleted lung cancer cells and employed to treat lung fibroblasts. The proliferation and migration of lung fibroblasts were investigated. The secretory genes were profiled in lung cancer cells upon *ARID1A* knockdown. Antibody-based neutralization was utilized to confirm their role in mediating the cross-talk between lung cancer cells and fibroblasts. NOD-SCID-IL2RgammaC-null (NSG) mice received tumor tissues from patients with *ARID1A*-mutated lung cancer to establish patient-derived xenograft (PDX) models. Notably, *ARID1A*-depleted lung cancer cells promoted the proliferation and migration of lung fibroblasts. Mechanistically, *ARID1A* depletion augmented the expression and secretion of prolyl 4-hydroxylase beta (P4HB) in lung cancer cells, which induced the activation of lung fibroblasts through the β -catenin signaling pathway. P4HB-activated lung fibroblasts promoted the proliferation, invasion, and chemoresistance in lung cancer cells. Neutralizing P4HB hampered the tumor growth and increased cisplatin cytotoxic efficacy in two PDX models. Serum P4HB levels were higher in *ARID1A*-mutated lung cancer patients than in healthy controls. Moreover, increased serum levels of P4HB were significantly associated with lung cancer metastasis. Together, our work indicates a pivotal role for P4HB in orchestrating the cross-talk between *ARID1A*-mutated cancer cells and cancer-associated fibroblasts during lung cancer progression. P4HB may represent a promising target for improving lung cancer treatment.

KEYWORDS

ARID1A, cancer-associated fibroblast, microenvironment, P4HB

Abbreviations: ARID1A, AT-interacting domain-rich protein 1A; CAF, cancer-associated fibroblast; EdU, ethynyldeoxyuridine; EMT, epithelial-mesenchymal transition; FAP, fibroblast activation protein; P4HB, prolyl 4-hydroxylase beta; PDI, protein disulfide isomerase; PDX, patient-derived xenograft; SWI/SNF, switch/sucrose non-fermentable; TME, tumor microenvironment; α -SMA, α -smooth muscle actin.

This is an open access article under the terms of the [Creative Commons Attribution-NonCommercial](https://creativecommons.org/licenses/by-nc/4.0/) License, which permits use, distribution and reproduction in any medium, provided the original work is properly cited and is not used for commercial purposes.

© 2023 The Authors. *Cancer Science* published by John Wiley & Sons Australia, Ltd on behalf of Japanese Cancer Association.

1 | INTRODUCTION

Lung cancer is one of the most lethal malignancies, with a 5 years overall survival rate of less than 20%.¹ Whole-genome sequencing studies have revealed the mutational landscape of lung cancer and shed light on cancer development and progression.² AT-interacting domain-rich protein 1A (*ARID1A*) gene is found to be frequently mutated in multiple human cancers including lung cancer.^{3–5} The mutations in *ARID1A* are mainly distributed throughout the coding region, resulting in a premature stop codon or frameshifts.³ Thus, inactivating *ARID1A* mutations often cause loss of *ARID1A* protein expression. As a key component of the switch/sucrose non-fermentable (SWI/SNF) complex, *ARID1A* functions as an epigenetic regulator to promote or repress gene transcription.⁴ In lung cancer, mutational inactivation of *ARID1A* promotes cancer cell proliferation and invasion and correlates with a poor prognosis.⁶ Loss of *ARID1A* in lung adenocarcinoma can facilitate tumorigenesis by enhancing glycolysis.⁵ These studies indicate that *ARID1A* mutation is a driving factor for lung cancer progression.

Cancer-associated fibroblasts (CAFs) are a key element of the tumor microenvironment (TME). The cross-talk between cancer cells and CAFs is indispensable for cancer development and progression.^{7–9} Cancer cells are capable of secreting lactate to drive CAF activation, which in turn promotes tumorigenesis.⁹ Colorectal cancer cells can release HSPC111 to modulate lipid metabolism in CAFs, consequently promoting liver metastasis.⁸ In lung cancer, CAFs can orchestrate various aspects of cancer biology, including proliferation, migration, invasion, epithelial–mesenchymal transition (EMT), and chemoresistance.^{10–12} Hence, understanding the reciprocal interactions between cancer cells and CAFs is of importance in developing effective therapeutic approaches for lung cancer.

Prolyl 4-hydroxylase beta (P4HB, also known as PDIA1) is a member of the protein disulfide isomerase (PDI) family. PDIs consist of multiple thioredoxin-like domains and can catalyze disulfide formation and isomerization in target proteins localized in the endoplasmic reticulum, thus modulating protein homeostasis.¹³ Previous studies have linked P4HB to cancer progression.^{14,15} It is aberrantly expressed in a variety of human cancers such as esophageal cancer,¹⁴ liver cancer,¹⁵ and lung cancer.¹⁶ Knockdown of P4HB attenuates the migration, invasion, and chemoresistance of liver cancer cells.¹⁵ In bladder cancer, silencing of P4HB increases the chemosensitivity to gemcitabine.¹⁷ However, the function of P4HB in lung cancer is still unclear.

It has been documented that *ARID1A* loss in cancer cells leads to remodeling of the immunosuppressive microenvironment.^{18,19} Mutation of *ARID1A* impairs T cell tumor infiltration and contributes to immune evasion.¹⁸ These findings encourage us to hypothesize that *ARID1A*-mutated cancer cells might regulate the activation of CAFs and establish a favorable niche for cancer progression. In the present study, we demonstrate that *ARID1A*-depleted lung cancer cells can promote lung fibroblast activation through secretion of P4HB. The P4HB-activated lung fibroblasts support a more aggressive phenotype in lung cancer cells.

2 | MATERIALS AND METHODS

2.1 | Cell culture

A549 and H1299 lung cancer cells were cultured in Dulbecco's modified Eagle medium (DMEM) supplemented with 10% fetal bovine serum (FBS; Invitrogen). MRC5 human lung fibroblasts were purchased from the American Type Culture Collection and cultured in Eagle's Minimum Essential Medium supplemented with 10% FBS (Sigma-Aldrich). Isolation of primary human lung fibroblasts was performed as described previously.²⁰ Briefly, fresh normal lung tissues adjacent to lung carcinoma tissues were obtained during surgery and minced to pieces. Then the tissue fragments were digested using 0.1% type I collagenase (Sigma-Aldrich) at 37°C. The mixture was cultured in DMEM/F12 with 10% FBS for 48h, and the unattached cells were removed. The adherent cells were collected as primary lung fibroblasts.

2.2 | *ARID1A* short hairpin RNAs (shRNAs), *CTNNB1* small interfering RNAs (siRNAs), and transfection

Two independent *ARID1A* shRNAs were cloned into the pLKO.1 puro vector, with the target sequences as follows: sh*ARID1A*#1: 5'-TAATG CCTTGCCCAATGCCAA-3'; sh*ARID1A*#2: 5'-ACATGACCTATAAT TATGCCA-3'. The *ARID1A* shRNAs were transfected into lung cancer cells using Lipofectamine 3000 (Invitrogen). Medium containing puromycin was used for selection of cells carrying *ARID1A* shRNAs. The sequences of the siRNAs used were as follows: si*CTNNB1*: 5'-GGAUGUUCACAACCGAAUUt-3'; siP4HB#1: 5'-CAGGACGGUCA UUGAUUACt-3'; siP4HB#2: 5'-AAGAUGAACUGUAUACGct-3'. The siRNAs were transfected using Lipofectamine 3000 at a final concentration of 40nM.

2.3 | Quantitative real-time PCR (qRT-PCR) analysis

Total RNA was isolated using the TRIzol reagent (Invitrogen) and converted to cDNA using the High-Capacity cDNA Reverse Transcription Kit (Invitrogen). Quantitative PCR reactions were done using the SYBR green reagent (Invitrogen) on an ABI Prism 7000HT sequence detection system. The PCR primer sequences are shown as follows:

ARID1A forward 5'-CCTGAAGAACTCGAACGGGAA-3', *ARID1A* reverse 5'-TCCGCCATGTTGTTGGTGG-3'; α -SMA forward 5'-TTACTACTGCTGAGCGTGAGATT-3', α -SMA reverse 5'-CTTCT CAAGGGAGGATGAGGATG-3'; *FAP* forward 5'-CCAGAATGTTT CGGTCTGT-3', *FAP* reverse 5'-CGAAATGGCATCATAGCTGA-3'; *P4HB* forward 5'-CTCGACAAAGATGGGGTGT-3', *P4HB* reverse 5'-GCAAGAACAGCAGGATGTGA-3'; *GAPDH* forward 5'-GGAGCGAG ATCCCTCCAAAAT-3', *GAPDH* reverse 5'-GGCTGTTGTCATACTTC

TCATGG-3'. Gene expression was determined after normalization to GAPDH.

2.4 | qRT-PCR array

qRT-PCR array was used to profile the expression of 84 genes that have the potential to encode secretory proteins and are involved in cancer progression. Briefly, cDNAs reverse transcribed from RNA samples were mixed with PCR master mix and subjected to qRT-PCR analysis. The relative mRNA expression levels were determined after normalization against five endogenous control genes.

2.5 | Western blot analysis

Whole-cell lysis was performed in radioimmunoprecipitation assay (RIPA) buffer supplemented with protease inhibitors (Beyotime Biotechnology). Equal amounts of protein were separated in sodium dodecyl sulfate-polyacrylamide gel electrophoresis and transferred to nitrocellulose membranes. Membranes were blocked in 5% fat-free milk and incubated overnight at 4°C with primary antibodies against ARID1A (Cell Signaling Technology), P4HB (Abcam), nonphospho (active) β -catenin (Cell Signaling Technology), β -catenin (Cell Signaling Technology), and GAPDH (Cell Signaling Technology). After washing, the membranes were incubated with appropriate horseradish peroxidase (HRP)-conjugated secondary antibodies (Cell Signaling Technology). The protein signals were probed using enhanced chemiluminescence reagents (Cell Signaling Technology).

2.6 | Preparation of conditioned medium

To prepare conditioned medium, 2×10^6 cells were cultured in serum-free medium for 24 h. The conditioned medium was collected, centrifuged, and filtered through a 0.22- μ m filter before use.

2.7 | Enzyme-linked immunosorbent assay (ELISA)

P4HB concentrations in the conditioned medium of cancer cells were measured using a commercially available ELISA kit according to the manufacturer's instructions (Abcam).

2.8 | Exogenous P4HB and anti-P4HB neutralizing antibody treatment

For P4HB treatment, MRC5 cells were exposed to different concentrations of recombinant P4HB protein (R&D Systems) and examined

for proliferation and migration. For neutralization of P4HB, a specific anti-P4HB antibody (10 ng/mL; Abcam) was added to the conditioned medium of cancer cells.

2.9 | Top/Fop-Flash luciferase reporter assay

To assess the β -catenin-dependent transcriptional activity, TOP/FOP-Flash luciferase reporter assay was performed as previously described.²¹ Briefly, the Top-Flash or Fop-Flash reporter and pTK-RL plasmids were cotransfected into MRC5 cells and treated with different concentrations of P4HB. After 24 h, the cells were lysed and tested for firefly and *Renilla* luciferase activities using the Dual-Luciferase Reporter Assay System (Promega). The Top/Fop ratio was calculated.

2.10 | Cell proliferation assay

For cell proliferation assay, 1×10^3 cells were seeded on 96-well plates and exposed to conditioned media. Cell viability was assessed every 24 h for up to 96 h using the MTT Cell Proliferation Kit (Sigma-Aldrich). The optical density of the formazan solutions was measured at a wavelength of 570 nm.

2.11 | Ethynyldeoxyuridine (EdU) incorporation assay

Proliferating cells were detected using the EdU Cell Proliferation Kit (Beyotime Biotechnology) according to the manufacturer's protocol. Briefly, cancer cells were seeded on the coverslips in 24-well plates and exposed to the conditioned medium of MRC5 cells for 24 h. The cells were incubated with 10 μ M EdU for 2 h and subjected to fixation, permeabilization, and staining for EdU. Nuclei were counterstained with Hoechst 33342 (Beyotime Biotechnology).

2.12 | Colony formation assay

Cancer cells were seeded on six-well plates (500 cells per well) and treated with the conditioned medium of MRC5 cells for 10–14 days. The colonies formed by cancer cells were counted.

2.13 | Transwell migration and invasion assay

For migration assays, 2×10^4 MRC5 cells in serum-free medium were plated into the upper chamber of a Transwell with polycarbonate filters. For invasion assays, 5×10^4 cancer cells in serum-free medium were plated into the upper chamber with

Matrigel-coated inserts. The medium containing 10% FBS was added to the lower chamber. After 24h, the cells that migrated to or invaded the lower chamber were stained with crystal violet and counted.

2.14 | In vitro cytotoxicity assay

Cancer cells were treated with different concentrations of cisplatin (Sigma-Aldrich) for 72h in the presence of MRC5 conditioned medium. Cell viability was determined using the MTT method.

2.15 | Analysis of P4HB concentrations in serum samples

Serum samples from 70 healthy individuals (50 males and 20 females, median age of 58 years) and 90 patients with *ARID1A*-mutated lung cancer (67 males and 23 females, median age of 57 years) were obtained. Among the lung cancer patients, 37 had metastatic disease. Serum P4HB concentrations were quantified by ELISA.

2.16 | Patient-derived xenograft (PDX) mouse models

For generation of PDX models,²² freshly resected tumor tissues were obtained from two patients with *ARID1A*-mutated lung cancer and minced to ~2mm³ tissue fragments. The two lung cancer patients did not receive any anticancer treatment before surgery. The tissue fragments were implanted subcutaneously in recipient male NOD-SCID-IL2RgammaC-null (NSG) mice (5 weeks old). When the xenograft tumors reached approximately 200mm³, the mice were randomly divided into four groups: the control group was injected with phosphate-buffered saline (PBS), the anti-P4HB group was injected intraperitoneally with anti-P4HB (100µg; once every 4 days for 16 days), the cisplatin group was injected intraperitoneally with cisplatin (5mg/kg; twice per week for 2 weeks), and the anti-P4HB+cisplatin group was injected intraperitoneally with anti-P4HB (100µg; once every 4 days for 16 days) and cisplatin (5mg/kg; twice per week for 2 weeks). Each group had five mice. The tumor volume was measured by caliper, and tumor growth curves were compared.

2.17 | Histological and immunohistochemical analysis

The xenograft tumor tissues were fixed in 4% paraformaldehyde for 48h, dehydrated, and embedded in paraffin. Deparaffined sections (4µm thickness) were stained using the Masson's Trichrome Stain Kit according to the manufacturer's protocol (Solarbio). After staining, the tissue sections were examined under a microscope. For immunohistochemical analysis, the sections were deparaffinized and treated with 3% hydrogen peroxide to eliminate endogenous peroxidase activity. The sections were then incubated with primary antibodies against α-SMA, Ki-67, TTF1, and PD-L1 (Cell Signaling Technology) for 2h, followed by appropriate secondary antibodies for 1h. The sections were washed and incubated in 3,3'-diaminobenzidine solution for 5min. The sections were counterstained with hematoxylin before microscopic examination.

2.18 | Statistical analysis

All results are expressed as mean±standard deviation. The statistical differences between the groups were determined by Student's t-test or one-way ANOVA and Tukey's post hoc test. A value of $p < 0.05$ was considered to be statistically significant.

3 | RESULTS

3.1 | *ARID1A*-depleted lung cancer cells promote lung fibroblast activation

The *ARID1A* gene is frequently mutated in patients with lung adenocarcinoma, and loss of *ARID1A* predicts poor prognosis.⁶ Animal studies have indicated the role of *ARID1A* inactivation in initiating metabolic reprogramming to drive lung tumorigenesis and progression.⁵ Given the fact that *ARID1A* loss in cancer cells can remodel the TME,^{18,19} we asked whether *ARID1A*-depleted lung cancer cells have an impact on lung fibroblast activation. To address this, we knocked down *ARID1A* expression in both A549 and H1299 lung cancer cells using lentiviral vectors expressing *ARID1A*-targeting shRNAs. Relative to the scrambled control cells, the mRNA level of *ARID1A* was reduced by over 70% in the *ARID1A* shRNA-transfected cells (Figure 1A). Western blot analysis confirmed the decreased protein level of *ARID1A* in the *ARID1A* shRNA-transfected cells

FIGURE 1 *ARID1A*-depleted lung cancer cells promote lung fibroblast activation. (A) qRT-PCR analysis of *ARID1A* mRNA levels in A549 and H1299 lung cancer cells transfected with control shRNA (shCtrl) or *ARID1A*-targeting shRNAs (sh*ARID1A*#1 and #2). * $p < 0.05$ compared with the shCtrl group. (B) Western blot analysis of *ARID1A* protein levels in the cells treated as in (A). (C) Analysis of the proliferation of MRC5 cells exposed to the conditioned medium (CM) of A549 (left) and H1299 (right) cells transfected with indicated shRNAs. * $p < 0.05$. (D) Representative images of the migration of MRC5 cells treated as in (C) using Transwell assays. Bar graphs (right) show the results from three independent experiments. * $p < 0.05$ compared with the shCtrl group. (E,F) Analysis of α-SMA and FAP mRNA levels in MRC5 cells (E) and primary lung fibroblasts (F) exposed to the conditioned medium of lung cancer cells transfected with indicated shRNAs. * $p < 0.05$ compared with the shCtrl group.

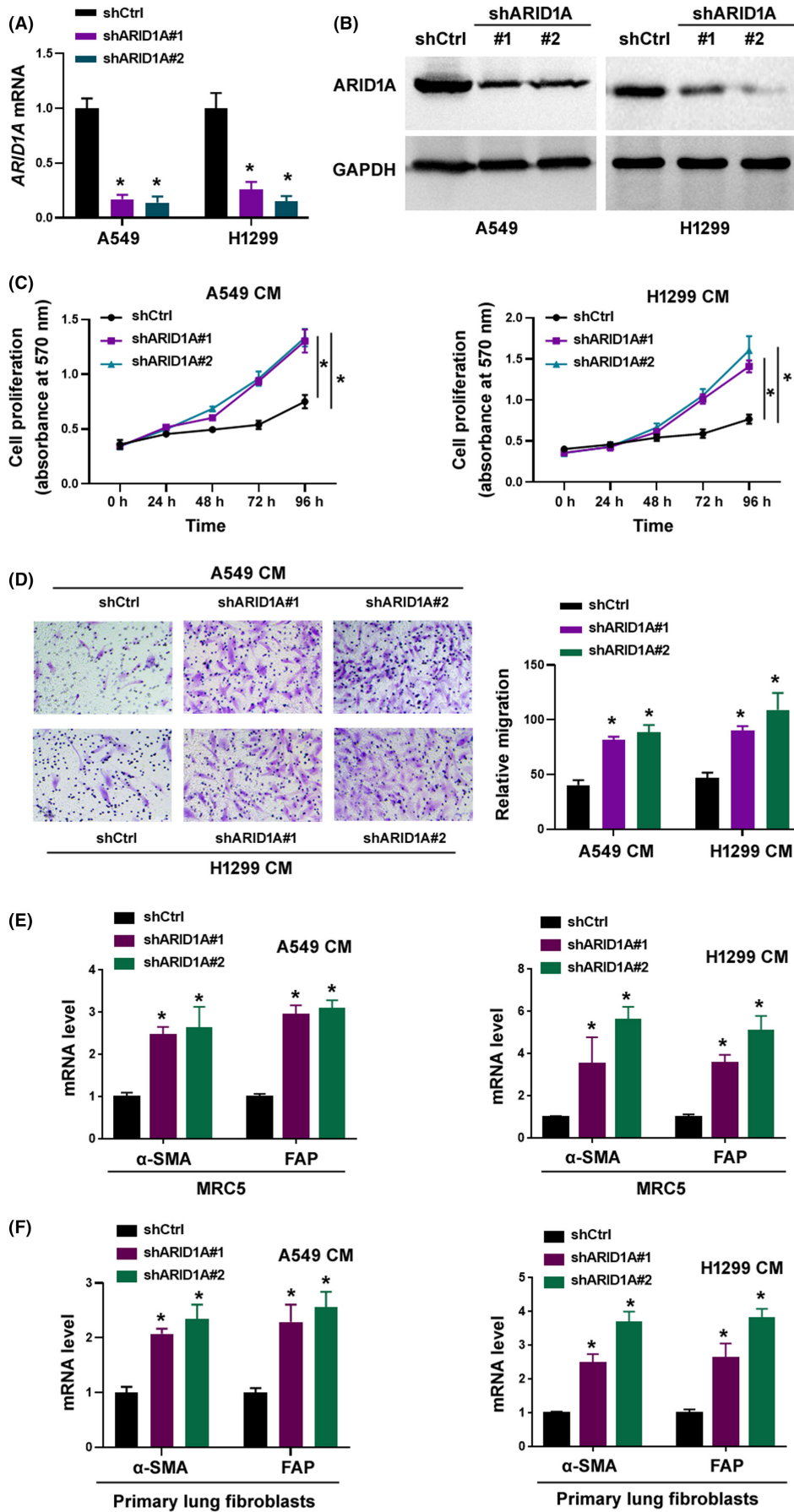


(Figure 1B). Next, the conditioned media of *ARID1A*-depleted lung cancer cells were harvested and used to treat MRC5 lung fibroblasts. Intriguingly, exposure to the conditioned media of *ARID1A*-depleted lung cancer cells led to an increase in the proliferation and migration of MRC5 cells (Figure 1C,D). Examination of CAF markers α -SMA and FAP demonstrated that treatment with the conditioned media of *ARID1A*-depleted lung cancer cells enhanced the expression of α -SMA and FAP in MRC5 cells (Figure 1E). Similarly, both α -SMA and FAP were induced in primary lung fibroblasts in response to the conditioned media of *ARID1A*-depleted lung cancer cells (Figure 1F). Taken together, these findings suggest that *ARID1A* loss renders lung cancer cells with an enhanced ability to stimulate lung fibroblast activation.

3.2 | P4HB upregulation upon *ARID1A* deficiency promotes lung fibroblast activation

To understand how *ARID1A* loss in lung cancer cells leads to the activation of lung fibroblasts, we conducted PCR array assays to profile 84 cancer-related mRNAs with the potential to encode secretory proteins. We found that upon *ARID1A* depletion, 17 were significantly regulated (Figure 2A). Among them, only *P4HB* expression was consistently upregulated in both the A549 and H1299 cells, which was corroborated by qRT-PCR and Western blot analyses (Figure 2B,C). Analysis of the conditioned media of *ARID1A*-depleted lung cancer cells further indicated that *ARID1A* silencing augmented the release of P4HB to the extracellular microenvironment (Figure 2D). Hence, P4HB is upregulated in response to *ARID1A* deficiency.

Next, we investigated the role of P4HB in the cross-talk between lung cancer cells and lung fibroblasts. To this end, we blocked the activity of P4HB in the conditioned media of *ARID1A*-depleted lung cancer cells using a specific P4HB neutralizing antibody. Notably, the neutralization of P4HB impaired the stimulation of MRC5 cell proliferation and migration by the conditioned media from *ARID1A*-depleted lung cancer cells (Figure 2E-G). Moreover, the effect of the conditioned media from *ARID1A*-depleted lung cancer cells on α -SMA and FAP expression in MRC5 cells was reversed by the neutralization of P4HB (Figure 2H,I). We also performed *P4HB* knockdown experiments in *ARID1A*-depleted lung cancer cells. As shown in Figure S1, depletion of *P4HB* rescued the effects of the conditioned media of *ARID1A*-depleted lung cancer cells on MRC5 cell proliferation and migration. Taken together, these findings suggest that *ARID1A*-depleted lung cancer cells direct lung fibroblast activation through the release of P4HB.

3.3 | P4HB-mediated phenotype in lung fibroblasts involves activation of the β -catenin signaling pathway

To further interrogate the role of P4HB in promoting lung fibroblast activation, we treated MRC5 fibroblasts with different concentrations of P4HB. We observed that exogenous P4HB caused a concentration-dependent upregulation of α -SMA and FAP in MRC5 cells (Figure 3A). The proliferation and migration of MRC5 cells was potentiated in the presence of exogenous P4HB (Figure 3B,C).

Previous studies have reported the involvement of β -catenin signaling in the induction of CAFs.^{23,24} Hence, we checked the effect of exogenous P4HB on the activation of β -catenin in lung fibroblasts. Interestingly, exposure to P4HB increased the levels of nonphosphorylated (active) β -catenin and enhanced β -catenin-dependent transcriptional activity (Figure 3D,E). Most importantly, knockdown of β -catenin attenuated the promotion of MRC5 cell proliferation and migration by exogenous P4HB (Figure 3F-H). Overall, these data indicate that the β -catenin signaling pathway is involved in P4HB-induced lung fibroblast activation.

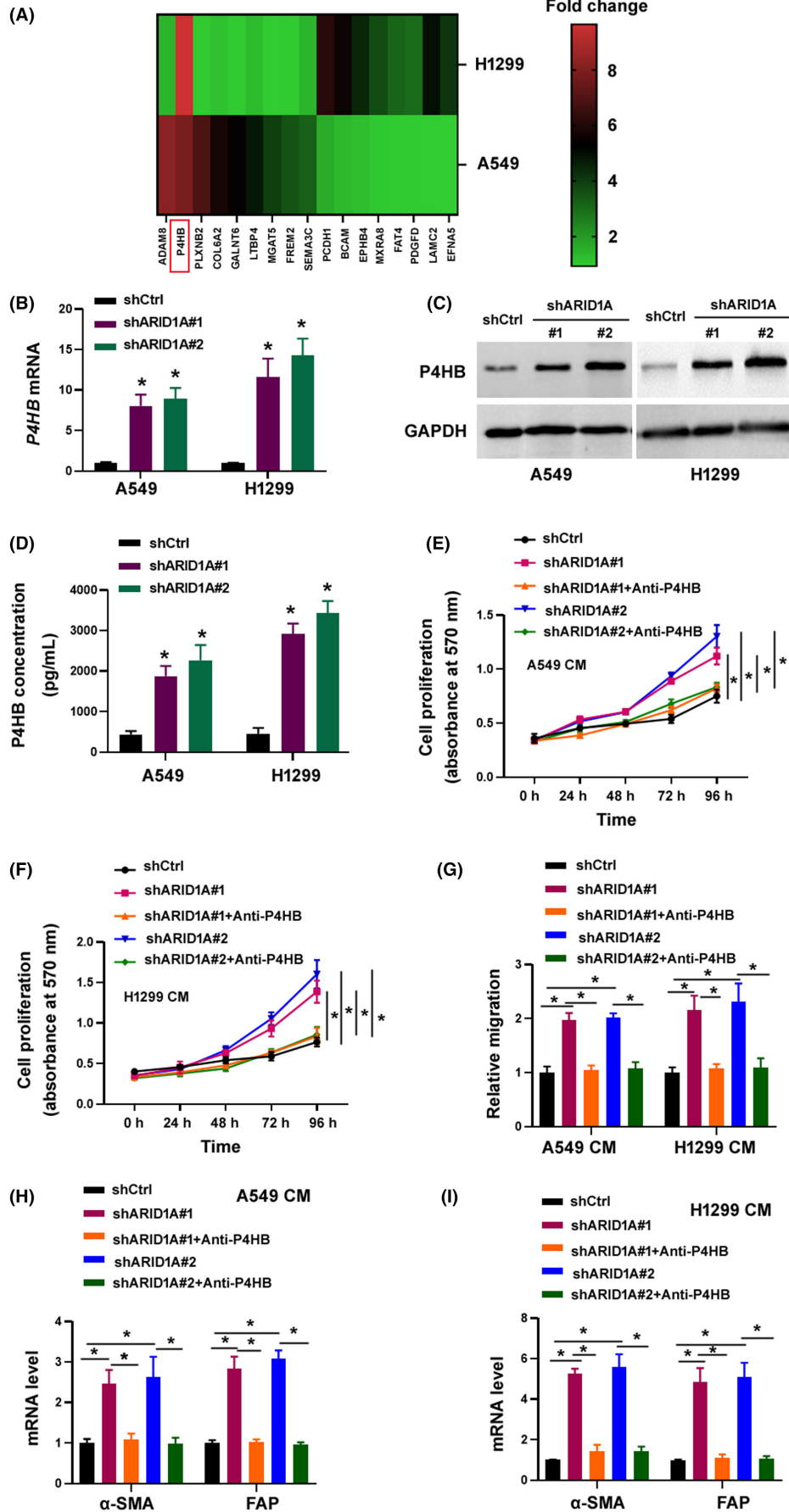
3.4 | P4HB-activated lung fibroblasts can enhance the aggressive property of lung cancer cells

Next, we determined the effect of P4HB-activated lung fibroblasts on lung cancer cells. MRC5 cells were treated with exogenous P4HB, and the conditioned media were collected. When A549 and H1299 lung cancer cells were exposed to the conditioned media from P4HB-activated MRC5 cells, their cell proliferation, colony formation, and invasion abilities were increased (Figure 4A-D). Moreover, treatment with the conditioned media from P4HB-activated MRC5 cells conferred cisplatin resistance to lung cancer cells (Figure 4E). These results suggest that P4HB-activated lung fibroblasts contribute to lung cancer progression and chemoresistance.

3.5 | Treatment of *ARID1A*-mutated lung cancer PDXs with anti-P4HB restrains tumor growth and increases chemosensitivity

Next, we checked whether neutralizing P4HB could yield therapeutic effects against lung cancer. To this end, we established *ARID1A*-mutated lung cancer PDXs in NSG mice. Like the corresponding primary tumors, the PDX tumors showed positive immunostaining for TTF1, a lung adenocarcinoma marker and PD-L1, a transmembrane

FIGURE 2 P4HB upregulation upon *ARID1A* deficiency promotes lung fibroblast activation. (A) Heatmap displays fold change of differentially expressed mRNAs detected by PCR array analysis in cancer cells transfected with indicated shRNAs. *P4HB* in red square was consistently upregulated in both the A549 and H1299 cells. (B,C) *P4HB* expression levels detected by qRT-PCR (B) and Western blot (C) analyses. * $p < 0.05$. (D) Quantification of the concentration of P4HB in the conditioned media of lung cancer cells transfected with indicated shRNAs. * $p < 0.05$. (E,F) Addition of anti-P4HB antibody blocked the stimulation of MRC5 cell proliferation by the conditioned media from *ARID1A*-depleted lung cancer cells. * $p < 0.05$. (G) Analysis of MRC5 cell migration after indicated treatments using Transwell migration assay. * $p < 0.05$. (H,I) Analysis of α -SMA and FAP mRNA expression in MRC5 cells after indicated treatments. * $p < 0.05$.



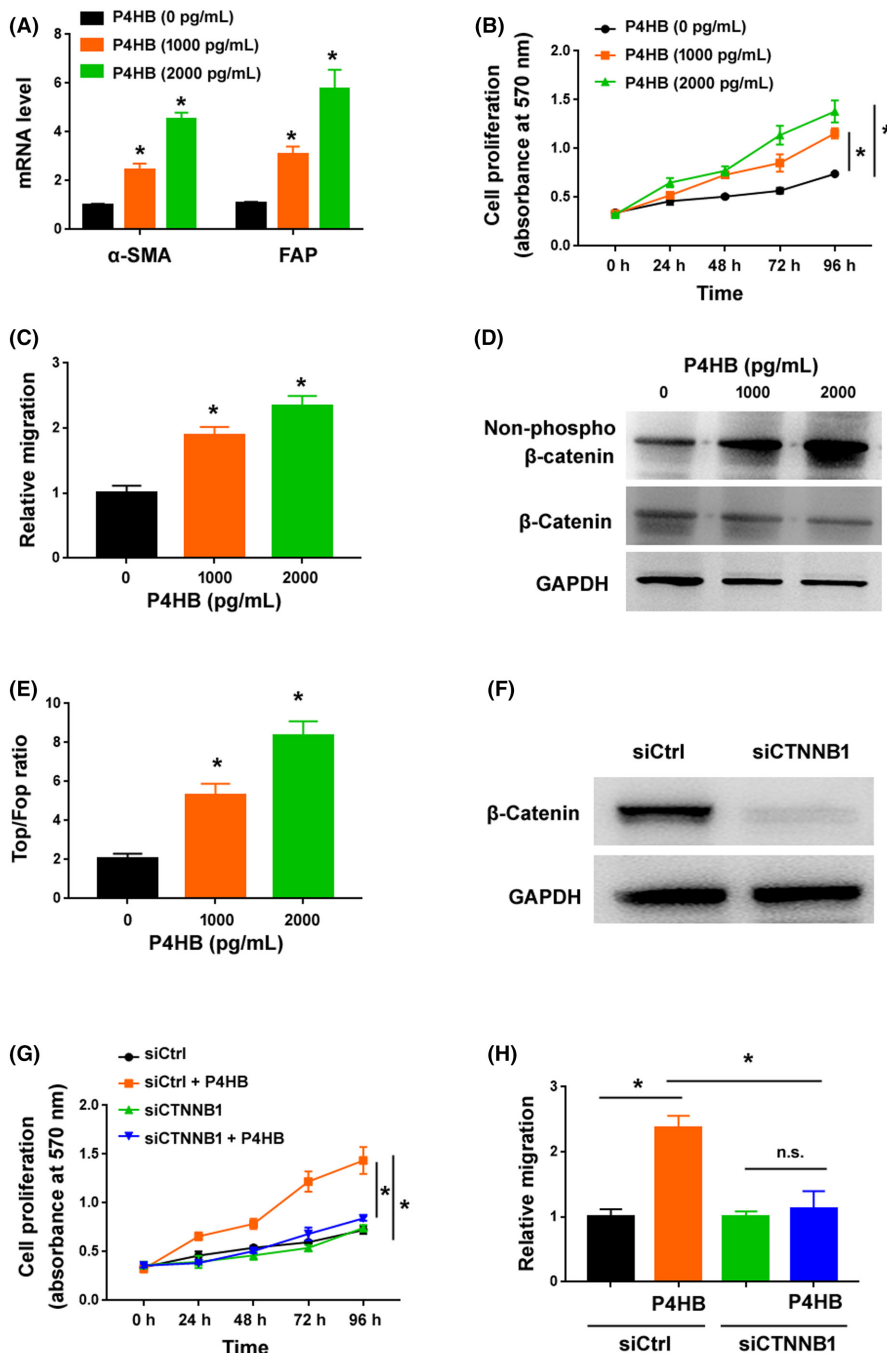
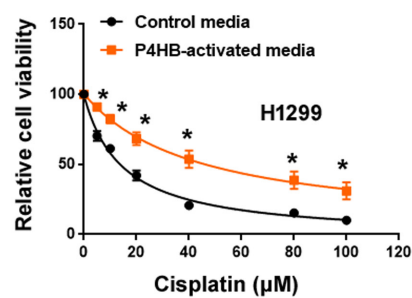
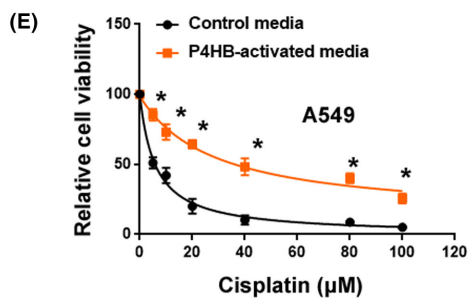
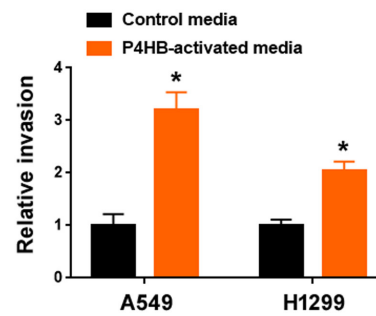
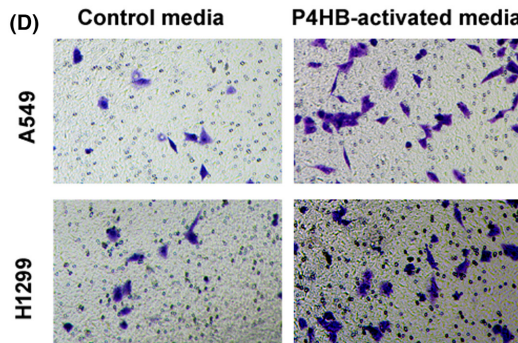
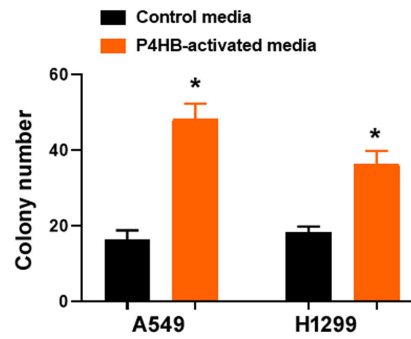
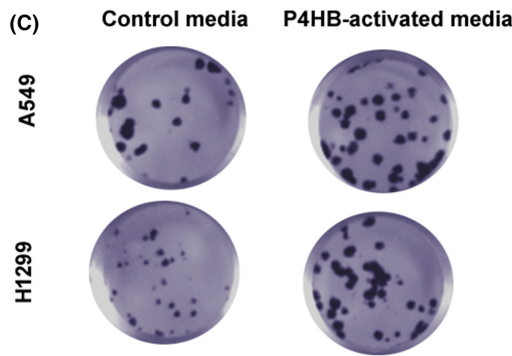
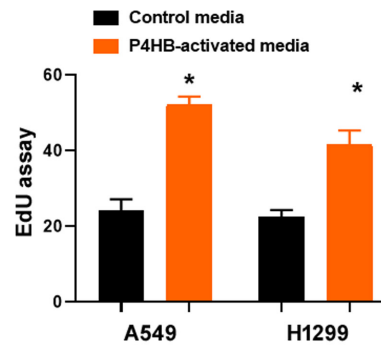
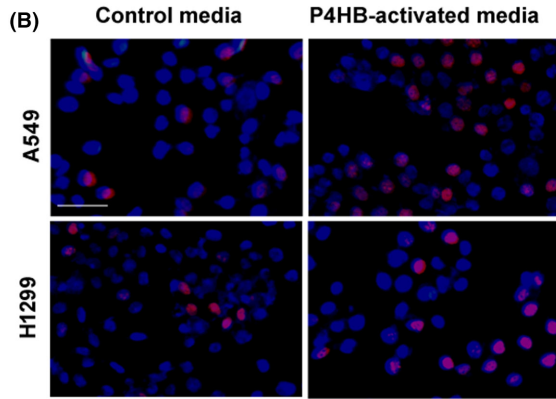
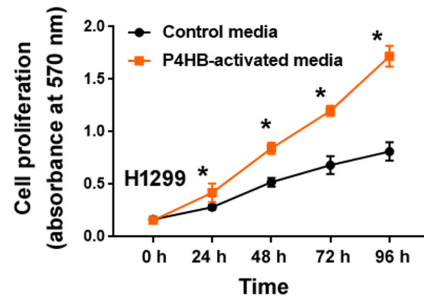
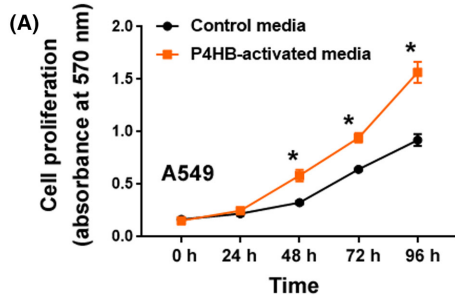


FIGURE 3 The β -catenin signaling pathway is involved in P4HB-induced lung fibroblast activation. (A) qRT-PCR analysis of α -SMA and FAP mRNA levels in MRC5 cells treated with different concentrations of P4HB. (B) Analysis of the proliferation of MRC5 cells treated with different concentrations of P4HB. (C) The migration of MRC5 cells treated with different concentrations of P4HB using Transwell migration assays. (D) Western blot analysis of nonphosphorylated (active) β -catenin levels in MRC5 cells treated with different concentrations of P4HB. (E) Top/Fop-Flash luciferase reporter assays performed to determine β -catenin-dependent transcriptional activity in MRC5 cells treated with different concentrations of P4HB. (F) Knockdown of *CTNNB1* in MRC5 cells transfected with control siRNA (siCtrl) or *CTNNB1*-targeting siRNA (siCTNNB1). (G) The proliferation and (H) migration of MRC5 cells after indicated treatments. * $p < 0.05$. n.s. indicates no significance.

ligand for immune checkpoint receptor PD1 (Figure 5A). The results showed that the PDX tumors preserved the histological characteristics and immune phenotype of the primary tumors. In the

two PDX models, administration of the anti-P4HB neutralizing antibody yielded a significant tumor growth inhibition (Figure 5B,C). Histological analysis confirmed a significant reduction of the CAF

FIGURE 4 P4HB-activated lung fibroblasts can enhance the aggressive property of lung cancer cells. (A) Analysis of the proliferation of A549 and H1299 cells exposed to the conditioned media from P4HB-activated MRC5 cells or control cells. * $p < 0.05$ compared with the control group. (B) EdU incorporation assay in A549 and H1299 cells exposed to the conditioned media from P4HB-activated MRC5 cells. Representative images (left) show EdU-positive cells (red). Scale bar = 50 μ m. * $p < 0.05$ compared with the control group. (C) Colony formation assay in A549 and H1299 cells exposed to the conditioned media from P4HB-activated MRC5 cells or control cells. Left, representative images from three independent experiments. * $p < 0.05$ compared with the control group. (D) Transwell invasion assay in A549 and H1299 cells exposed to the conditioned media from P4HB-activated MRC5 cells or control cells. Left, representative images from three independent experiments. * $p < 0.05$ compared with the control group. (E) A549 and H1299 cells were exposed to the conditioned media from P4HB-activated MRC5 cells or control cells and treated with different concentrations of cisplatin. The cell viability was measured 72 h after treatment. * $p < 0.05$ compared with the control group.



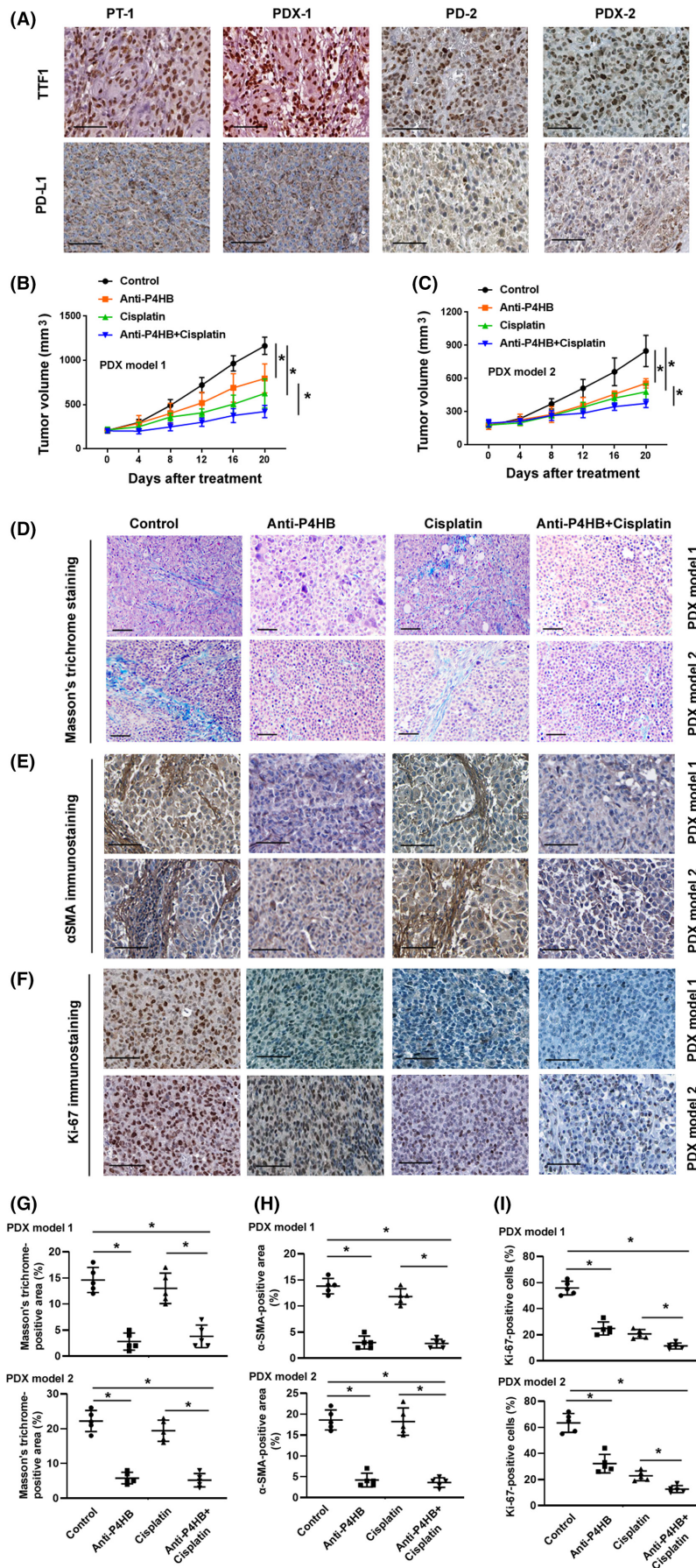


FIGURE 5 Treatment of *ARID1A*-mutated lung cancer patient-derived xenografts (PDXs) with anti-P4HB restrains tumor growth and increases chemosensitivity. (A) Immunohistochemical analysis of TTF1 and PD-L1 expression in two PDX models and their corresponding primary tumors (PTs). Scale bar = 100 μ M. (B,C) Analysis of the therapeutic effects of anti-P4HB neutralizing antibody alone or in combination with cisplatin on two *ARID1A*-mutated lung cancer PDX models in NSG mice (five mice per group). * $p < 0.05$. (D) Masson's trichrome staining of tumor sections from two PDX models after indicated treatments. Scale bar = 100 μ M. (E,F) Immunohistochemical staining for (E) α -SMA and (F) Ki-67 in tumor sections from two PDX models after indicated treatments. Scale bar = 100 μ M. (G) Quantification of Masson's trichrome-positive area ($n = 5$). * $p < 0.05$. (H,I) Quantification of (H) α -SMA and (I) Ki-67 staining in tumor sections ($n = 5$). * $p < 0.05$.

population (Figure 5D,E,G,H) and Ki-67-positive proliferating tumor cells (Figure 5F,I) in the anti-P4HB group relative to the control group. Moreover, combined treatment with anti-P4HB antibody and cisplatin caused an enhancement of the growth suppression and CAF reduction in the *ARID1A*-mutated PDXs (Figure 5B-I). These results suggest that blocking P4HB activity may represent an effective therapeutic strategy against *ARID1A*-mutated lung cancer.

3.6 | Clinical significance of serum P4HB in lung cancer

Compared with healthy controls, patients with *ARID1A*-mutated lung cancer had significantly higher concentrations of serum P4HB (Figure 6A). Moreover, serum P4HB levels were significantly associated with metastasis in patients with *ARID1A*-mutated lung cancer (Figure 6B). These results suggest that serum P4HB may serve as a biomarker for lung cancer progression.

4 | DISCUSSION

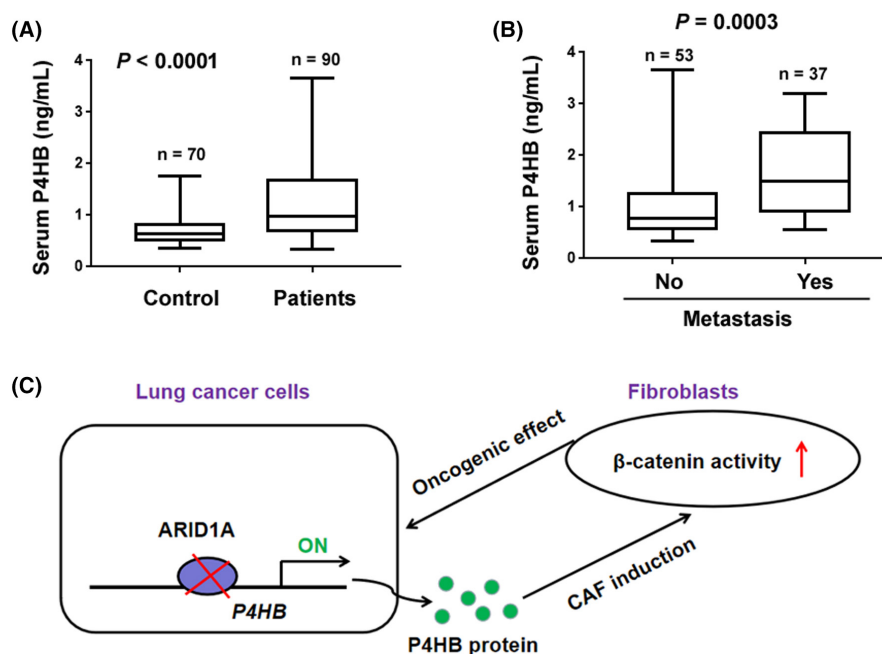
In this study, we demonstrate that *ARID1A*-depleted lung cancer cells can stimulate the activation of lung fibroblasts, probably through secretion of inductive factors to the extracellular microenvironment. Exposure to the conditioned media from *ARID1A*-depleted lung cancer cells induces a CAF-like phenotype in lung fibroblasts, upregulating CAF markers and increasing cell proliferation and migration. Reciprocal interactions between *ARID1A*-mutated cancer cells and immune cells in the TME have been reported.^{18,19} *ARID1A*-deficient cancer cells result in activation of NF- κ B signaling and consequential promotion of polymorphonuclear myeloid-derived suppressor cell chemotaxis, which contributes to immune evasion.¹⁹ Our results

highlight the ability of *ARID1A*-deficient cancer cells to trigger the activation of CAFs. Therefore, *ARID1A* loss may enable lung cancer cells to shape the TME, which supports tumor progression.

Our data further show that P4HB expression is significantly increased in lung cancer cells upon *ARID1A* loss. As an epigenetic regulator, *ARID1A* can modulate downstream gene transcription through multiple mechanisms including chromatin remodeling, histone modification, and alteration of DNA methylation status.^{25,26} As the *P4HB* transcript level was found to be elevated in *ARID1A*-deficient lung cancer cells, we suggest that the upregulation of P4HB may be the consequence of *ARID1A* loss-mediated epigenetic regulation. Overexpression of P4HB frequently occurs in human cancers.¹⁴⁻¹⁶ P4HB can orchestrate different cancer cell behaviors, including EMT, chemoresistance, tumorigenesis, proliferation, and invasion.^{15,17,27,28} Of note, P4HB can be secreted to the extracellular space. For example, it has been reported that P4HB is externalized by endothelial cells, consequently contributing to thrombosis and vascular remodeling.²⁹ Besides nonmalignant cells, our results show that *ARID1A*-deficient cancer cells can secrete P4HB to the extracellular space. Moreover, P4HB shows the ability to promote the activation of lung fibroblasts. When P4HB in the conditioned media from *ARID1A*-deficient lung cancer cells was blocked by the P4HB neutralizing antibody, the promotion of lung fibroblast activation by *ARID1A*-deficient lung cancer cells was impaired. Hence, we propose that extracellular P4HB may mediate the cross-talk between lung cancer cells and CAFs (Figure 6C).

Mechanistical studies reveal that P4HB induces lung fibroblast activation through the β -catenin signaling pathway. Exposure to P4HB results in the activation of β -catenin signaling in lung fibroblasts. Moreover, knockdown of β -catenin antagonizes P4HB-induced lung fibroblast activation. Our results indicate the dependence on the β -catenin signaling pathway for P4HB-induced lung fibroblast activation. This is consistent with a previous study

FIGURE 6 Clinical significance of serum P4HB in lung cancer. (A) Serum P4HB levels in patients with *ARID1A*-mutated lung cancer and healthy controls. (B) Serum P4HB levels in *ARID1A*-mutated lung cancer patients with or without metastatic disease. (C) Model for the cross-talk between *ARID1A*-mutated lung cancer cells and cancer-associated fibroblasts. *ARID1A*-mutated lung cancer cells can release P4HB to activate the β -catenin signaling pathway in cancer-associated fibroblasts. P4HB-activated lung fibroblasts can promote lung cancer cell growth, invasion, and chemoresistance.



where P4HB can regulate the β -catenin/Snai1 pathway in liver cancer cells.¹⁵ However, it remains to be clarified how P4HB in the TME of lung cancer signals to lung fibroblasts and drives the activation of the β -catenin signaling pathway.

Many studies have reported that CAFs support cancer progression by modulating cancer cell proliferation, migration, invasion, EMT, and chemoresistance.^{10–12} Our results suggest that the P4HB-activated lung fibroblasts resemble functionally CAFs. When lung cancer cells were treated with the conditioned media from P4HB-activated lung fibroblasts, they acquired a more aggressive phenotype. Overall, P4HB plays a crucial role in driving lung cancer progression. In agreement with these in vitro findings, clinical studies show that serum P4HB levels are increased in patients with *ARID1A*-mutated lung cancer and associated with metastasis. The prognostic significance of P4HB has been observed in several other malignancies including glioma and clear cell renal cell carcinoma.^{30,31} Thus, serum P4HB may have the potential as a biomarker in lung cancer management.

Cancer-associated fibroblasts are regarded as a potential therapeutic target for cancer treatment, because of the cross-talk between CAFs and cancer cells.^{32,33} Targeting CAFs has been found to improve therapeutic resistance in human cancers.^{34,35} Our data show the therapeutic potential of targeting P4HB in the treatment of *ARID1A*-mutated lung cancer. In particular, administration of the anti-P4HB neutralizing antibody restrained the growth of *ARID1A*-mutated lung cancer PDXs in NSG mice. Moreover, blocking P4HB potentiated the cytotoxic effect of cisplatin on the *ARID1A*-mutated PDXs. Our results provide a rationale for targeting the cross-talk between cancer cells and CAFs in the treatment of *ARID1A*-mutated lung cancer.

In summary, our data show that P4HB is upregulated in lung cancer cells upon *ARID1A* depletion and mediates the reciprocal interactions between lung cancer cells and CAFs. Serum P4HB holds promise as a useful biomarker for *ARID1A*-mutated lung cancer. Our findings underscore the importance of extracellular P4HB in lung cancer progression. Neutralizing P4HB represents a potential therapeutic approach for lung cancer.

AUTHOR CONTRIBUTIONS

Risheng Huang: Conceptualization; investigation; methodology; validation; writing – original draft. **Danni Wu:** Investigation; methodology. **Kangliang Zhang:** Data curation; investigation; methodology. **Guanqiong Hu:** Investigation; methodology; resources. **Yu Liu:** Investigation; methodology; software; validation. **Yi Jiang:** Methodology; resources; software; validation. **Chichao Wang:** Formal analysis; investigation; validation. **Yuanliang Zheng:** Conceptualization; data curation; formal analysis; funding acquisition; project administration; supervision; writing – review and editing.

ACKNOWLEDGMENTS

None.

FUNDING INFORMATION

This work was supported by the Natural Science Foundation of Zhejiang Province, China (LY21H160011 and LQ22H160024), Collaborative Education Project of Industry University Cooperation of the Ministry of Education of China (202101160012), and Key Laboratory of Precision Medicine of Wenzhou of China (2021HZSY0065).

CONFLICT OF INTEREST STATEMENT

The authors declare that they have no competing interests.

ETHICS STATEMENT

Approval of the research protocol by an institutional reviewer board: The experimental protocols involving human specimens were approved by the Institutional Review Board of Wenzhou Medical University (Wenzhou, China).

Informed consent: Each participant gave written informed consent. Registry and registration no. of the study/trial: N/A.

Animal studies: The animal experiments were performed in accordance with institutional guidelines and approved by the Institutional Animal Care and Use Committee of Wenzhou Medical University.

ORCID

Risheng Huang  <https://orcid.org/0009-0000-4880-847X>

REFERENCES

- Adams SJ, Stone E, Baldwin DR, Vliegenthart R, Lee P, Fintelman FJ. Lung cancer screening. *Lancet*. 2023;401:390-408.
- Chen J, Yang H, Teo ASM, et al. Genomic landscape of lung adenocarcinoma in east Asians. *Nat Genet*. 2020;52:177-186.
- Jones S, Wang TL, LeM S, et al. Frequent mutations of chromatin remodeling gene *ARID1A* in ovarian clear cell carcinoma. *Science*. 2010;330:228-231.
- Xu G, Chhangawala S, Cocco E, et al. *ARID1A* determines luminal identity and therapeutic response in estrogen-receptor-positive breast cancer. *Nat Genet*. 2020;52:198-207.
- Liu X, Li Z, Wang Z, et al. Chromatin remodeling induced by *ARID1A* loss in lung cancer promotes glycolysis and confers JQ1 vulnerability. *Cancer Res*. 2022;82:791-804.
- Sun D, Zhu Y, Zhao H, et al. Loss of *ARID1A* expression promotes lung adenocarcinoma metastasis and predicts a poor prognosis. *Cell Oncol (Dordr)*. 2021;44:1019-1034.
- Yuan M, Tu B, Li H, et al. Cancer-associated fibroblasts employ NUFIP1-dependent autophagy to secrete nucleosides and support pancreatic tumor growth. *Nat Cancer*. 2022;3:945-960.
- Zhang C, Wang XY, Zhang P, et al. Cancer-derived exosomal HSPC111 promotes colorectal cancer liver metastasis by reprogramming lipid metabolism in cancer-associated fibroblasts. *Cell Death Dis*. 2022;13:57.
- Linares JF, Cid-Diaz T, Duran A, et al. The lactate-NAD⁺ axis activates cancer-associated fibroblasts by downregulating p62. *Cell Rep*. 2022;39:110792.
- Wang Y, Lan W, Xu M, et al. Cancer-associated fibroblast-derived SDF-1 induces epithelial-mesenchymal transition of lung adenocarcinoma via CXCR4/ β -catenin/PPAR δ signalling. *Cell Death Dis*. 2021;12:214.

11. Lee S, Hong JH, Kim JS, et al. Cancer-associated fibroblasts activated by miR-196a promote the migration and invasion of lung cancer cells. *Cancer Lett.* 2021;508:92-103.
12. Su S, Chen J, Yao H, et al. CD10+GPR77+ cancer-associated fibroblasts promote cancer formation and Chemoresistance by sustaining cancer Stemness. *Cell.* 2018;172:841-856.
13. Matsusaki M, Kanemura S, Kinoshita M, Lee YH, Inaba K, Okumura M. The protein disulfide isomerase family: from proteostasis to pathogenesis. *Biochim Biophys Acta Gen Subj.* 2020;1864:129338.
14. Gao X, Wang Y, Lu F, et al. Extracellular vesicles derived from oesophageal cancer containing P4HB promote muscle wasting via regulating PHGDH/Bcl-2/caspase-3 pathway. *J Extracell Vesicles.* 2021;10:e12060.
15. Ma X, Wang J, Zhuang J, et al. P4HB modulates epithelial-mesenchymal transition and the β -catenin/snail pathway influencing chemoresistance in liver cancer cells. *Oncol Lett.* 2020;20:257-265.
16. Wang SM, Lin LZ, Zhou DH, Zhou JX, Xiong SQ. Expression of prolyl 4-hydroxylase beta-polypeptide in non-small cell lung cancer treated with Chinese medicines. *Chin J Integr Med.* 2015;21:689-696.
17. Wang X, Bai Y, Zhang F, et al. Targeted inhibition of P4HB promotes cell sensitivity to gemcitabine in urothelial carcinoma of the bladder. *Onco Targets Ther.* 2020;13:9543-9558.
18. Li J, Wang W, Zhang Y, et al. Epigenetic driver mutations in ARID1A shape cancer immune phenotype and immunotherapy. *J Clin Invest.* 2020;130:2712-2726.
19. Li N, Liu Q, Han Y, et al. ARID1A loss induces polymorphonuclear myeloid-derived suppressor cell chemotaxis and promotes prostate cancer progression. *Nat Commun.* 2022;13:7281.
20. Yang F, Yan Y, Yang Y, et al. MiR-210 in exosomes derived from CAFs promotes non-small cell lung cancer migration and invasion through PTEN/PI3K/AKT pathway. *Cell Signal.* 2020;73:109675.
21. Kim WK, Kwon Y, Jang M, et al. β -Catenin activation down-regulates cell-cell junction-related genes and induces epithelial-to-mesenchymal transition in colorectal cancers. *Sci Rep.* 2019;9:18440.
22. Peng Q, Chen L, Wu W, et al. EPH receptor A2 governs a feedback loop that activates Wnt/ β -catenin signaling in gastric cancer. *Cell Death Dis.* 2018;9:1146.
23. Liu T, Zhou L, Yang K, et al. The β -catenin/YAP signaling axis is a key regulator of melanoma-associated fibroblasts. *Signal Transduct Target Ther.* 2019;4:63.
24. Ferrari N, Ranftl R, Chicherova I, et al. Dickkopf-3 links HSF1 and YAP/TAZ signalling to control aggressive behaviours in cancer-associated fibroblasts. *Nat Commun.* 2019;10:130.
25. Yamada H, Takeshima H, Fujiki R, et al. ARID1A loss-of-function induces CpG Island methylator phenotype. *Cancer Lett.* 2022;532:215587.
26. Guo B, Friedland SC, Alexander W, et al. Arid1a mutation suppresses TGF- β signaling and induces cholangiocarcinoma. *Cell Rep.* 2022;40:111253.
27. Xia W, Zhuang J, Wang G, Ni J, Wang J, Ye Y. P4HB promotes HCC tumorigenesis through downregulation of GRP78 and subsequent upregulation of epithelial-to-mesenchymal transition. *Oncotarget.* 2017;8:8512-8521.
28. Sun S, Kiang KMY, Ho ASW, et al. Endoplasmic reticulum chaperone prolyl 4-hydroxylase, beta polypeptide (P4HB) promotes malignant phenotypes in glioma via MAPK signaling. *Oncotarget.* 2017;8:71911-71923.
29. Araujo TLS, Zeidler JD, Oliveira PVS, Dias MH, Armelin HA, Laurindo FRM. Protein disulfide isomerase externalization in endothelial cells follows classical and unconventional routes. *Free Radic Biol Med.* 2017;103:199-208.
30. Zhu Z, He A, Lv T, Xu C, Lin L, Lin J. Overexpression of P4HB is correlated with poor prognosis in human clear cell renal cell carcinoma. *Cancer Biomark.* 2019;26:431-439.
31. Sun S, Kiang KM, Leung GK. Chaperone protein P4HB predicts temozolomide response and prognosis in malignant glioma. *Oncol Lett.* 2022;24:264.
32. Chen Y, McAndrews KM, Kalluri R. Clinical and therapeutic relevance of cancer-associated fibroblasts. *Nat Rev Clin Oncol.* 2021;18:792-804.
33. Affo S, Nair A, Brundu F, et al. Promotion of cholangiocarcinoma growth by diverse cancer-associated fibroblast subpopulations. *Cancer Cell.* 2021;39:866-882.
34. Zhang H, Deng T, Liu R, et al. CAF secreted miR-522 suppresses ferroptosis and promotes acquired chemo-resistance in gastric cancer. *Mol Cancer.* 2020;19:43.
35. Galbo PM Jr, Zang X, Zheng D. Molecular features of cancer-associated fibroblast subtypes and their implication on cancer pathogenesis, prognosis, and immunotherapy resistance. *Clin Cancer Res.* 2021;27:2636-2647.

SUPPORTING INFORMATION

Additional supporting information can be found online in the Supporting Information section at the end of this article.

How to cite this article: Huang R, Wu D, Zhang K, et al. ARID1A loss induces P4HB to activate fibroblasts to support lung cancer cell growth, invasion, and chemoresistance. *Cancer Sci.* 2024;115:439-451. doi:[10.1111/cas.16052](https://doi.org/10.1111/cas.16052)